JOURNAL OF PROPULSION AND POWER
Vol. 11, No. 3, May–June 1995

Gasdynamic Fusion Propulsion System for Space Exploration

Terry Kammash* and Myoung-Jae Lee†
University of Michigan, Ann Arbor, Michigan 48109

An open-ended fusion system in which a high-density plasma is confined and heated to thermonuclear temperatures is examined as a potential high specific power propulsion device that can be used for space exploration. With a collision mean free path much smaller than a characteristic dimension of the system, the plasma behaves much like a continuous medium (fluid) for which the confinement time is drastically different from that which characterizes a typical fusion power reactor. Noting that fact and using an appropriate set of balance equations we derive an expression for the length of the rocket in terms of the plasma parameters required for certain propulsive capabilities. We find that a moderately sized system can produce large values of specific impulse and thrust that would allow a massive rocket to make a round-trip to Mars in months instead of years. By carrying out a preliminary engineering design we also identify those technological areas that must be developed before such a system can become practical. Many of these technologies are surprisingly not out of reach today.

Nomenclature

A_c = central region area
A_0 = mirror cross-sectional area; nozzle area
B_p = magnetic field in plasma
B_{p0} = vacuum magnetic field
C_m = engineering design safety factor
c = velocity of light
c_0 = constant defined in Eq. (9)
D = one-way linear distance ($=D_{ab}$, D_{ba})
E = electron energy in Eq. (19)
E_{in} = injection energy
E_L = escape energy
E_s = magnet stored energy
E_0 = energy produced by fusion
F = thrust
g = Earth's gravitational acceleration
I_{sp} = specific impulse
J = current density
k = constant defined in Eq. (9)
L = length of rocket
M_m = magnet mass
M_{rad} = radiator mass
M_{ref} = refrigerator mass
M_s = shield mass
M_{tot} = total mass ($=M_m + M_{rad} + M_{ref} + M_s$)
m = ion mass
m_b = $m_f + m_p^{b\to a}$
m_f = dry mass of vehicle
m_i = initial mass of vehicle
$m_p^{b\to a}$ = mass of propellant used in traveling from b to a
m_0 = rest mass of electron
N = factor defined in Eq. (16)
n = plasma density
P_b = bremsstrahlung power
P_f = fusion power
P_{in} = injected power
P_R = plasma pressure
P_s = synchrotron radiation power
Q = reactor gain factor
q = ion charge
R = plasma mirror ratio
R_c = reflection coefficient
R_0 = vacuum mirror ratio
r_M = mirror (throat) radius in Fig. 1
r_m = radius to magnet in Fig. 1
r_p = plasma radius in Fig. 1
r_s = radius to outer wall of shield in Fig. 1
r_w, r_s = inner and outer radii of shield in Fig. 1
r_0 = classical electron radius
r_1, r_2 = inner and outer radii of conductor
S = injection rate per cm^3
T = plasma temperature
U_B = magnetic energy density
V_m = volume enclosed by magnetic field
v = velocity
v_{th} = thermal velocity
W_f = dry weight of vehicle
α, α^* = mass ratios defined in Eqs. (26–30)
β = ratio of plasma pressure to magnetic field pressure
γ = ratio of specific heats
δ = fraction occupied by J
θ = loss cone angle
λ = collision mean free path
μ_0 = magnetic permeability
ρ_i = ion Larmor radius
ρ_m = magnet mass density
ρ_s = structure density
τ = confinement time
τ_{RT} = round-trip travel time
σ_s = stress in structure
σ_T = Thompson cross section
$\langle\sigma v\rangle$ = velocity averaged fusion cross section
ω_{ci} = ion gyrofrequency

Received Oct. 8, 1993; revision received April 14, 1994; accepted for publication Aug. 26, 1994.
*Professor of Nuclear Engineering. Associate Fellow AIAA.
†Graduate Student in Nuclear Engineering.

Introduction

ONE of the most critical ingredients of a manned mission to the planet Mars is a propulsion system that can make the trip in a relatively short time to minimize physical degradation and exposure to hazardous galactic radiation by the crew. The device we consider in this article is such a system, and consists of a solenoid around which a current-carrying conductor is wound to generate a "simple mirror" magnetic geometry in which a hot plasma is confined and allowed to undergo fusion reactions. The system, shown in Fig. 1, is maintained in steady state by injection of particles in the region of the homogeneous magnetic field to effectively balance the plasma loss through the mirrors, where the magnetic field is stronger than it is at the center. If we denote by R_0

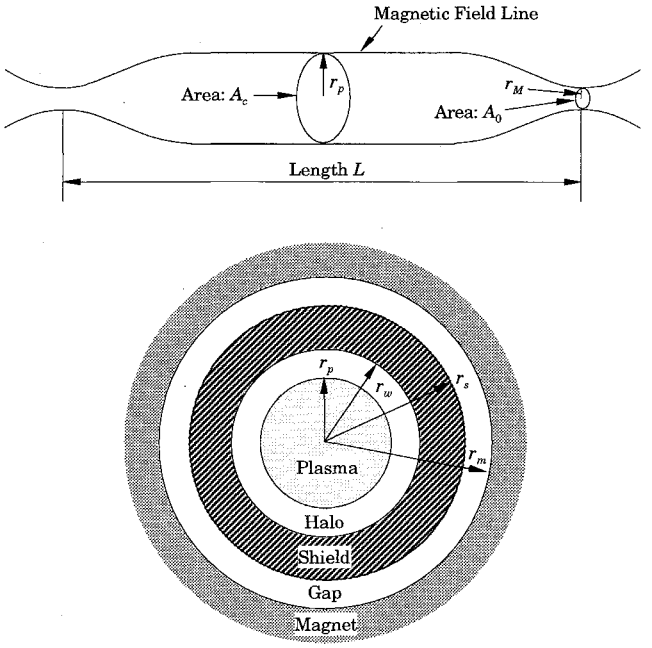

Fig. 1 Schematic and cross-sectional view of the gasdynamic fusion propulsion system.

the ratio of the vacuum field at the mirror to that at the center, then as a propulsion system asymmetry in the mirror ratios must be imposed in order to minimize losses through the mirror that will not be used as a nozzle. In fact, for a device with a large aspect ratio ($L >> r_p$), the magnetic configuration is effectively that of a "meridional" nozzle,[1] which is azimuthally symmetric in that the fluid flow velocity is everywhere parallel to the magnetic field lines. In contrast to a conventional mirror fusion reactor where a typical fuel ion will traverse the device several times before it undergoes a scattering collision,[2] the plasma in the propulsion system will be sufficiently dense so that λ will be significantly smaller than a characteristic dimension of the system, i.e., the plasma will behave much like a continuous medium—a fluid. Under these circumstances the escape of the plasma from the system is analogous to the flow of a gas into a vacuum from a vessel with a hole. The plasma "flux" across the mirror cross section A_0 can be estimated as $A_0 n v_{\text{th}}$. By dividing the total number of particles in the system, $A_c nL$ (A_c is the cross-sectional area of the plasma in the central region) by the flux we can find the particle lifetime in the device to be

$$\tau \sim (A_c L / A_0 v_{\text{th}}) = RL/v_{\text{th}} \tag{1}$$

where R (related to R_0) is the mirror ratio seen by the plasma. A more accurate derivation of the confinement time and the mean energy E_L of an escaping ion can be obtained by noting that the velocity distribution of the particles in a fluid is Maxwellian, hence,

$$\frac{1}{\tau} = \frac{4}{\sqrt{\pi}}\left(\frac{m}{2T}\right)^{3/2} \int_0^\infty \frac{v}{RL} v^2 e^{-mv^2/2T}\, dv = \frac{1}{RL}\sqrt{\frac{8T}{\pi m}} = \frac{v_{\text{th}}}{RL} \tag{2}$$

$$\frac{E_L}{\tau} = \frac{4}{\sqrt{\pi}}\left(\frac{m}{2T}\right)^{3/2} \int_0^\infty \frac{mv^5}{2RL} e^{-mv^2/2T}\, dv = \frac{2T}{RL}\sqrt{\frac{8T}{\pi m}} = \frac{2Tv_{\text{th}}}{RL} \tag{3}$$

It follows therefore that

$$E_L = 2T \tag{4}$$

In contrast with the classical mirror where $\lambda >> L$, the lifetime is a linear, rather than a logarithmic, function of R. Consequently, in a gasdynamic confinement system, increasing the mirror ratio to the highest value permitted by the technology provides a much greater effect than in a classical mirror. For reasons that will become clear shortly, in this article we consider systems for which $R >> 1$. It might be added at this point that when $R >> 1$, the estimate given by Eq. (1) is valid when $\lambda/R << L$, which is much less stringent than the condition $\lambda << L$. In other words the quantity to be compared with the length of the device L is not the mean free path λ, but an effective mean free path against scattering through an angle of the order of the "loss cone" angle $\theta \sim 1/\sqrt{R}$. This angle represents a region in velocity space, which if a particle falls in it as a result of a Coulomb collision with another particle, it will definitely escape through the end. Under these conditions, any loss cone instability[3] arising from depletion of the velocity distribution function will not have an important effect on the longitudinal confinement time. Any reduction in the scattering length cannot cause a significant change in the rate at which the plasma is lost through the mirrors; thus, it cannot lower the lifetime below the value given in Eq. (1) or (2). In our assessment of this system as a propulsion device we must, however, strike a balance between its confinement capability as reflected in its ability to produce fusion energy to heat the fuel, and its propulsive capability as reflected in its ability to eject energetic particles through the mirror nozzle.

Another important feature of this system is the high plasma density in the region just beyond the mirror where it is comparable to that at the center of the system. This feature makes it possible to suppress the "flute" instability,[4] which is known to plague "classical" axisymmetric mirrors. Stability against this magnetohydrodynamic (MHD) mode and the loss cone microinstability alluded to above, provide an added dimension to the utility of this concept as propulsion device. In other words, there seems to be no serious plasma oscillation problems that could endanger the performance of the gasdynamic mirror as a propulsive system while it produces the fusion energy needed to heat its fuel (propellant). Moreover, since the presence of the plasma anywhere in the device reduces the magnetic field at that point, it follows that R seen by the plasma can be expressed in terms of R_0 by

$$R = R_0/(\sqrt{1-\beta}) \tag{5}$$

where

$$\beta = \sum nT/(B_{p0}^2/8\pi), \qquad B_p = B_{p0}\sqrt{1-\beta} \tag{6}$$

and B_{p0} is the vacuum field at the center. The quantity β is a measure of how effective the magnetic field is in confining the plasma, and its value is very sensitive to the MHD stability raised earlier. The more stable the system is against these modes, the higher beta value that can be sustained, and in turn, the higher the fusion power density that can be supported by the system.

In order to fully assess the performance of the gasdynamic mirror propulsion system, we must first establish the dynamics of the plasma it contains. Furthermore, we will carry out a preliminary engineering design in order to identify the critical areas of research and development that must be addressed before such a system can become operational. Moreover, such consideration allows us to assess the impact of confinement physics on the sizes and masses of these components as well as the demands placed on their performance capabilities. No attempt will be made to provide detailed or optimized design

of these parts since the technology in many instances may be viewed as still evolving. The physics model we employ is somewhat simplified in that we use one ion species to represent the deuterium-tritium (D-T) (50-50% mixture) ions with an average mass of 2.5 atomic mass units, and ignore the dynamics of the electron component of the plasma as well as the alpha particles generated by the D-T fusion reactions. We shall assume a high β operation of the system arising from a large degree of plasma stability; that in turn allows us to assess the impact of reduced synchrotron radiation losses, especially in cases where high reflectivity R_e walls are assumed. Under these conditions the equations of interest reduce to the steady-state mass conservation equation

$$S - (n/\tau) - (n^2/2)\langle\sigma v\rangle = 0 \tag{7}$$

and the steady-state power (energy) balance equation

$$SE_{in} + (n^2/4)\langle\sigma v\rangle E_0 - (nE_L/\tau) - P_b - P_s = 0 \tag{8}$$

In these equations S is the rate of injection of fuel ions per unit volume, $\langle\sigma v\rangle$ the velocity-averaged fusion reaction cross section, E_{in} the energy of the injected particle, E_0 the energy produced by a D-T fusion reaction (17.6 MeV), P_b the bremsstrahlung radiation power, P_s the synchrotron radiation power and E_L the mean energy of an escaping ion. We recall from Eq. (4) that such an ion leaves with an average energy equal to twice the thermal energy of a confined ion. It is convenient to express many of the terms in the conservation equations explicitly in terms of the temperature, i.e., to write

$$\begin{aligned} n &= \frac{B_{p0}^2\beta}{16\pi T} = \frac{B_{p0}^2}{kT}, \qquad k \equiv \frac{16\pi}{\beta} \\ \frac{1}{\tau} &= \frac{T^{1/2}}{c_0 RL}, \qquad c_0 \equiv \sqrt{\frac{\pi m}{8}} \\ P_b &= p_0 n^2 T^{1/2} = \frac{p_0 B_{p0}^4}{k^2} T^{-3/2} \\ P_s &= s_0 n^2 T^2 = \frac{s_0 B_{p0}^4}{k^2} \end{aligned} \tag{9}$$

where $p_0 = 3.34 \times 10^{-15}$ keV$^{1/2}$ cm^3/s and s_0 is given by Eq. (20). The quantity $\langle\sigma v\rangle$ is also temperature-dependent, but since this dependence varies in different temperature regimes, it will be left in its standard form until numerical evaluations are called for. If we solve for S from Eq. (7) and substitute the result in Eq. (8) we obtain an expression for the plasma (device) length as a function of temperature, i.e.,

$$L = \frac{kT(E_{in} - 2T)}{B_{p0}^2 c_0 R[p_0 + s_0 T^{3/2} - \frac{1}{4}\langle\sigma v\rangle(2E_{in} + E_0)T^{-1/2}]} \tag{10}$$

which upon insertion of the first of Eq. (9) becomes

$$L = \frac{(E_{in} - 2T)}{nc_0 R[p_0 + s_0 T^{3/2} - \frac{1}{4}\langle\sigma v\rangle(2E_{in} + E_0)T^{-1/2}]} \tag{11}$$

The value of E_{in} can be established by first noting that the injection power P_{in} can be expressed in terms of P_f through Q of the reactor. Using the standard definition of Q, we can write

$$(n^2/4)\langle\sigma v\rangle E_0/(nE_{in}/\tau) = Q \tag{12}$$

which upon substituting from the second of Eq. (9), and utilizing Eq. (11) we find

$$E_{in} = -\frac{\xi}{4} + \sqrt{\left(\frac{\xi}{4}\right)^2 + \frac{E_0 E_L}{2Q}} \tag{13}$$

where

$$\xi = E_0\left(\frac{1}{Q} + 1\right) - \frac{4(P_b + P_s)}{n^2\langle\sigma v\rangle}$$

In fact, it can readily be shown that if the radiation terms are ignored the injection energy can be simply expressed by

$$E_{in} \approx E_L/(Q + 1) = 2T/(Q + 1) \tag{14}$$

which clearly indicates that a lower injection energy will be needed if the reactor is to produce power in excess of the amount required to sustain it. For a propulsion system where the injected power is balanced exactly by the fusion power (i.e., $Q = 1$), the injection energy of Eq. (13) can be put into Eq. (11), and upon noting further that p_0, s_0, and E_{in} can be neglected in comparison with E_0, the device length can be approximated by

$$L \approx 4T^{3/2}/nc_0 R\langle\sigma v\rangle E_0 \tag{15}$$

It is perhaps worth noting at this point that a study carried out several decades ago on a hypothetical fusion propulsion rocket vehicle,[5] also utilized a mirror fusion scheme as the basic configuration. Unlike the concept considered in this article, the mirror of the hypothetical rocket made use of a "collisionless" plasma in a mirror geometry, taking advantage of the properties generated by the fusion research of that era. One such property is the stable confinement (against the flute instability) provided by the "cusp" or "minimum B" geometry obtained when current-carrying conductors (Ioffee bars) were superimposed on the standard mirror-field generating coils. No plasma dynamic equations were, however, used in that study; instead a minimum ion confinement time was deduced based on the premise that the energy carried away by the mass flow cannot exceed the total net reactor power, or the fusion reactions would be extinguished. Not only is this approach too rudimentary, but it also fails to give the proper dependence on ion temperature as well as to include in the confinement time the mirror ratio that is the hallmark of mirror confinement physics. Although considerable detail was devoted to the design aspects of the various components of the system, the results must be viewed with some caution due to the deficient physics model used in obtaining these values.

Plasma Parameters and Elementary Design Considerations

Because of the dependence of $\langle\sigma v\rangle$ on temperature, Eq. (11) or (15) reveals that the length minimizes at a particular temperature, and that such a length decreases with increasing plasma density and mirror ratio. Theses facts are displayed in Fig. 2. We also note from Fig. 3 that the length is smallest for a rocket that operates at the breakeven condition, i.e., at $Q = 1$. For the case at hand the minimization occurs near $T = 20$ keV, but operating at this temperature and at a desirable density depends critically on whether the confining magnetic field is technologically feasible. For example, if we choose a high value of β commensurate with the high degree of plasma stability (noted earlier), e.g., $\beta = 0.95$, the value of the vacuum magnetic field at the center of the device needed to support a plasma with a density of 10^{16} cm^{-3} and a temperature of 20 keV is about 13 T. This may be at the edge of present day technology. On the other hand the vacuum field at the mirror end will, according to Eq. (5), be about 145 T, which may well be beyond today's reach. It should be noted, however, that these magnetic field values will be significantly higher if, for one reason or another, a smaller value of β is found to be dictated by the physics of the system. Such a problem will be further exacerbated when we realize that such fields, especially in the uniform region, must be extended over

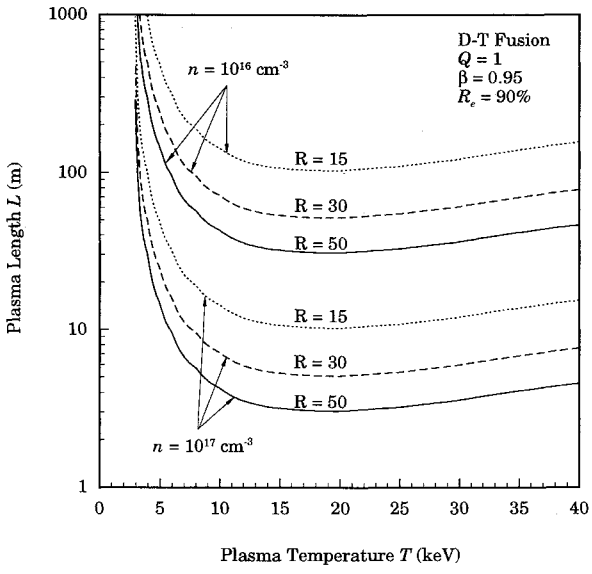

Fig. 2 Effect of mirror ratio on plasma (rocket) length.

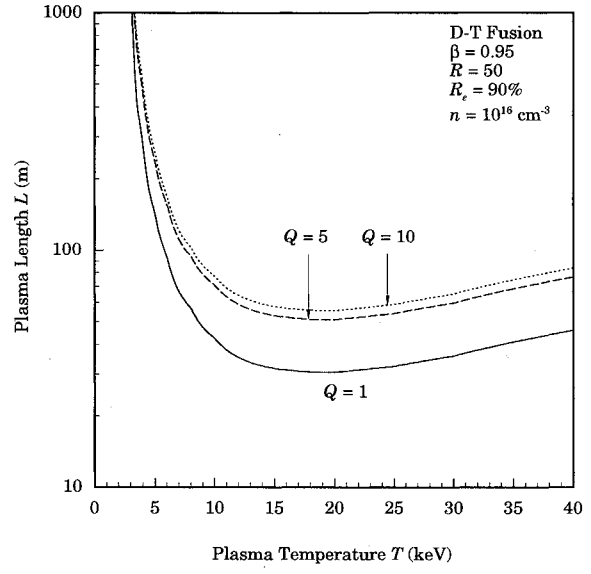

Fig. 3 Role of reactor gain factor in plasma (rocket) size.

long distances, of the order of the length of the rocket. Although such large fields have been achieved in some current fusion experiments, the plasma in these devices generally do not extend over comparable distances.

In choosing r_p, we must, on the one hand, insure that it is larger than the fuel ion gyroradius so that it is confined by the magnetic field in that region, and on the other, insure that the area at the nozzle (mirror) is adequate to produce a thrust power commensurate with an attractive specific power for the rocket. If we denote by N the ratio of r_p to ρ_i, where the latter is the ion gyroradius, then

$$r_p = N\rho_i = N(v_{\text{thi}}/\omega_{ci}), \qquad \omega_{ci} = qB/mc \tag{16}$$

With the aid of Eq. (6) we can readily write

$$r_p(\text{cm}) = 0.72N\sqrt{T_i(\text{keV})}/B_{p0}\ (\text{T})\sqrt{1-\beta} \tag{17}$$

A midsection plasma radius of about 7 cm at a magnetic field of 13 T, which confines a plasma with $n = 10^{16}$ cm^{-3}, and $T = 20$ keV at $\beta = 0.95$ yields by the above equation an N value of about 6 while a radius of 21.2 cm for the same plasma yields $N = 19$, indicating in both instances that confinement needs are met. If we use Eq. (1) we find that the radii at the mirror (nozzle) for these two cases are 1 and 3 cm, respectively, yielding correspondingly areas of 3.14 cm^2 and 28.26 cm^3. As noted earlier, the magnetic geometry for such a long and slender device is that of a meridional nozzle for which the thrust is expressed by[1]

$$F \cong \gamma A_0 P_R = \gamma A_0 \sum nT \tag{18}$$

where $\gamma = 5/3$ is the ratio of specific heats, A_0 the nozzle area, $\Sigma\, nT$ the P_R in the central region (reservoir), and the sum is over the ion and electron components of the plasma. For the example cited above, Eq. (18) yields about 33 kN in the case of $A_0 = 3.14$ cm^2, and about 300 kN of thrust for $A_0 = 28.26$ cm^2. At a temperature of 20 keV the mean exhaust velocity of the ions is about 1.76×10^6 m/s, which yields a specific impulse of about 1.79×10^5 s. However, if we include the electron contribution we find that the effective exhaust velocity of the fuel is about 1.78×10^5 m/s, yielding an effective I_{sp} of about 1.82×10^5 s.

Of special interest is the rate of the synchrotron radiation in the performance of the system, and the impact it may have on the design of some of the major components. Though often ignored compared to the bremsstrahlung (X-ray) radiation especially in cases where the plasma temperature and the strength of the magnetic field are relatively small, the radiative loss by this process in the present case could be significant. If we denote by R_e the reflection coefficient of the walls surrounding the plasma, then the synchrotron radiation power density can be expressed in a relativistically correct form as[6]

$$\left(\frac{dE}{dt}\right)_{\text{syn}} = \frac{4nT}{m_0 c}\,\sigma_T U_B \left(1 + \frac{5T}{2m_0c^2}\right)(1 - R_e) \tag{19}$$

where

$$\sigma_T = \frac{8}{3}\pi r_0^2 = \frac{8}{3}\pi\left(\frac{e^2}{m_0c^2}\right)$$

$$U_B = \frac{B_{p0}^2}{8\pi}$$

and $m_0c^2 = 511$ keV is the rest mass energy of the electron, and $r_0 = 2.818 \times 10^{-13}$ cm, the classical electron radius. In writing the above expression we have assumed that the electron density and temperature are the same as those of the ions. Making use of the definition of β, and inserting the various numerical constants, Eq. (19) can be put in the form:

$$\left(\frac{dE}{dt}\right)_{\text{syn}} = \frac{5.002 \times 10^{-38}}{\beta}\, n^2\,(\text{m}^{-3})\, T^2\,(\text{keV}) \times \left[1 + \frac{T\,(\text{keV})}{204}\right](1 - R_e) \tag{20}$$

We note that the radiated power decreases as $\beta \to 1$, because the plasma effectively shields the electrons from the magnetic field, and a perfectly reflecting wall completely prevents the escape of this radiation. Figure 4 shows that the length of the device as a function of the plasma temperature is not affected significantly by the loss or retention of the synchrotron radiation, but it will be seen later that this radiated power can indeed impact the size of the radiator, and correspondingly the specific power of this propulsion system.

A major component in the engineering system of this propulsion device is the magnet that provides the confinement of the plasma. To calculate its mass we examine three plausible scenarios that progress from present day/near future

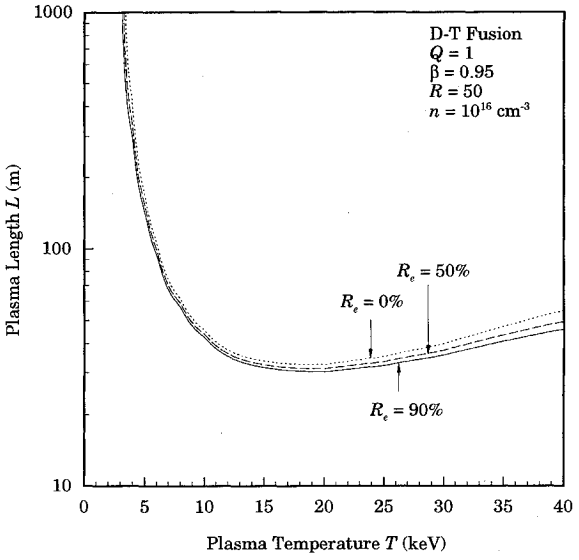

Fig. 4 Wall reflection of synchrotron radiation and its effect on length.

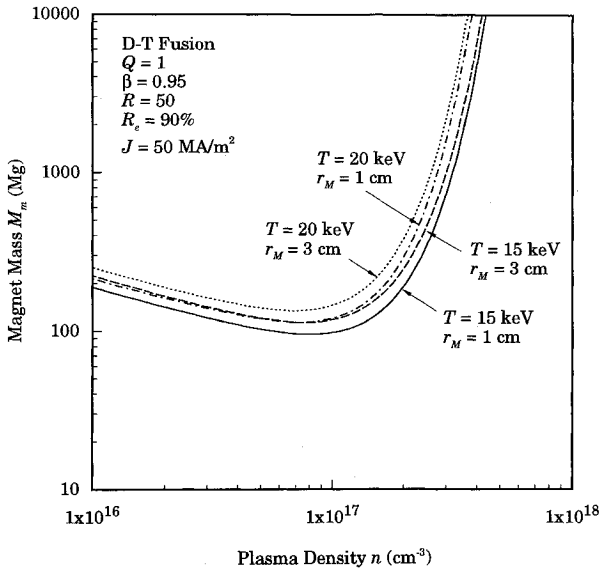

Fig. 5 Magnet mass for different mirror radii and plasma temperature for near term technology.

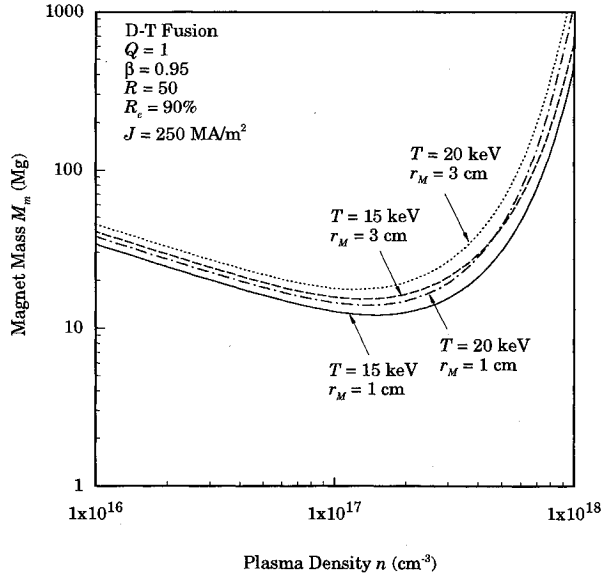

Fig. 6 Magnet mass for different mirror radii and plasma temperature with advanced technology.

technology to an advanced superconducting technology, to an approach that makes use of the magnetic virial theorem.[7] In the first two estimates we make use of the winding-pack current density values of 50 and 250 MA/m^2, respectively. For a solenoid of length L, and an inner and outer radii of r_1 and r_2, respectively, the magnetic field strength at the center is given by[8]

$$B = \mu_0 \delta J \frac{L}{2} \ln\left[\frac{r_2 + (r_2^2 + L^2/4)^{1/2}}{r_1 + (r_1^2 + L^2/4)^{1/2}}\right] \tag{21}$$

where δ is the fraction of the coil volume occupied by the current-carrying conductor, and J the current density. By inserting the value of B needed to confine the plasma in the center, i.e., B_{p0}, and r_1 from the design given in Fig. 1, the outer radius can be calculated using the proposed values of J and L as well as an assumed δ, e.g., 0.90. The magnet mass then becomes

$$M_m = \pi L(r_2^2 - r_1^2)\rho_m \tag{22}$$

where ρ_m is about 6 mg/m^3. If material properties constitute the major limiting factor then the virial theorem might be applicable. It makes use of this constraint and suggests for the magnet mass the following value:

$$M_m = C_m(\rho_s/\sigma_s)E_s \tag{23}$$

where $C_m \cong 2$ is an engineering design safety factor, ρ_s the density of the structure (~2.5 mg/m^3 for carbon/carbon composite structure), σ_s the allowable stress (assumed to be 1000 MPa), and E_s is the stored energy in the magnet given by

$$E_s = (B^2/2\mu_0)V_m \tag{24}$$

Here, V_m is the volume enclosed by the magnetic field, i.e., $\pi r_m^2 L$ in the present case. Figures 5 and 6 show the magnet mass as a function of density for two different temperatures, and two mirror (nozzle) radii for current densities of 50 and 250 MA/m^2, respectively. Once again, we note that minimal mass occurs for a plasma density of 10^{-17} cm^{-3}, and for the lower temperatures and mirror radii. For example, the magnet mass at $n = 10^{17}$ cm^{-3}, $T = 15$ keV, $J = 50$ MA/m^2, and mirror radius of 1 cm is about 98 mg, and increases to 117 mg when the radius is increased to 3 cm while the other parameters remain the same. If the plasma temperature is increased to 20 keV while the other parameters remain the same, then the magnet mass for the 1 and 3 cm radius cases become, respectively, 120 and 144 mg. If advanced superconducting technology is achieved so that a current density of $J = 250$ MA/m^2 can be supported then the magnet masses of the last example will be replaced by 14.5 and 18 Mg, respectively. When the virial theorem is applied to the same case, the values become 15 and 22 mg, which are not drastically different from the superconducting magnet results.

Most of the fusion energy of 17.6 MeV appears in the neutron that carries 14.1 MeV, while the remainder is carried by the alpha particle, the second reaction product of D-T fusion. This large amount of energy along with the portion that appears in radiation (bremsstrahlung and synchrotron) will eventually manifest itself as heat and must be disposed of by a radiator. The mass of such a radiator is obtained by dividing this combined power by the power rejected per unit mass of this component, which is often taken to be 5 MW/mg. If we take the example of the system that utilizes a superconducting magnet (i.e., $J = 250$ MA/m^2) with a plasma with a density of 10^{17} cm^{-3}, and a temperature of 20 keV that

produces thrust through a 3 cm nozzle, then the radiator for such a propulsion device will have a mass of 20,992 mg, which is indeed quite large. Moreover, from a materials standpoint it is interesting to note that the wall loading on the surface surrounding the plasma due to neutron power in the above example is about 1725 MW/m^2, whereas the surface heat flux due to the radiated power is about 30 MW/m^2. Even with a superconducting magnet, some refrigeration will be needed for cooling purposes, and although that is difficult to estimate, it is reasonable to assume that its mass is about one-third that of the magnet. For the case at hand it is about 15 mg. To protect the magnet from the radiation emanating from the plasma, a shield must be interposed between these two regions as illustrated in Fig. 1. With a shield mass density of 1 mg/m^3, and the volume it occupies in the proposed design we find that its mass for the example under consideration is about 42 mg. When all of these masses are added together, the "dry" mass of the rocket is obtained, which for the present example amounts to 21,094 mg—a truly large system. Even with such a mass we will see shortly that a round-trip to Mars using this fusion rocket will take a relatively short time. Since the figure of merit for any propulsion device is its specific power, i.e., the power it delivers per unit mass, the effective thrust power for our example is about 5.4 $\times$ 10^5 MW, yielding a specific power of about 26 kW/kg.

Because of the sensitivity of travel time to the total mass of the vehicle, it is important to identify the parameters that tend to make it smaller. Figure 7, which may be viewed as embodying a near-term design consideration of this propulsion concept, reveals that a plasma density between 10^{15}–10^{16} cm^{-3} minimizes the mass for the temperatures and mirror radii under consideration, with the smaller temperature and smaller radius being more desirable. Figure 8 gives the same information for a more futuristic design, which assumes an advanced magnet technology that fully utilizes a current density of 250 MA/m^2 in its magnet design. Minimization of the mass by the various parameters is similar to the previous case, but as expected the minimum total mass is smaller in this case due to the smaller magnet mass produced by superconductivity. If the virial theorem of magnet design is employed then the results are displayed in Fig. 9 where similar profiles are obtained. A comparison of the three approaches is depicted in Fig. 10. It should be kept in mind, however, that as important as reducing the total mass is, it should be reconciled with the propulsion parameters that the device produces and their impact on travel time. This will be examined in the next section.

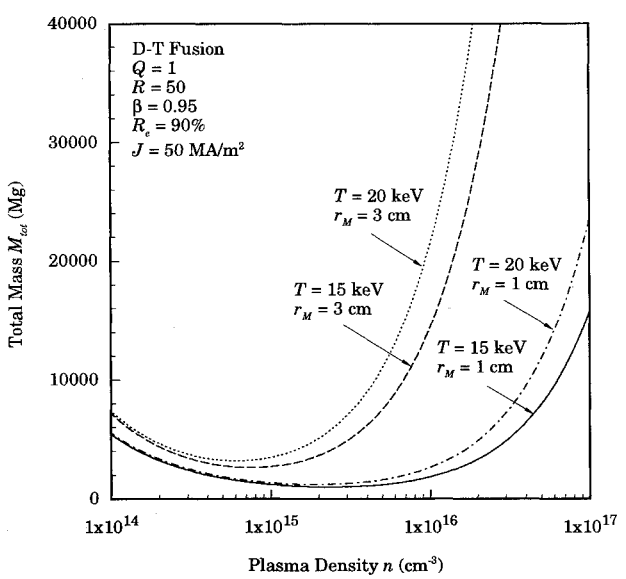

Fig. 7 Total rocket mass at near term magnet technology.

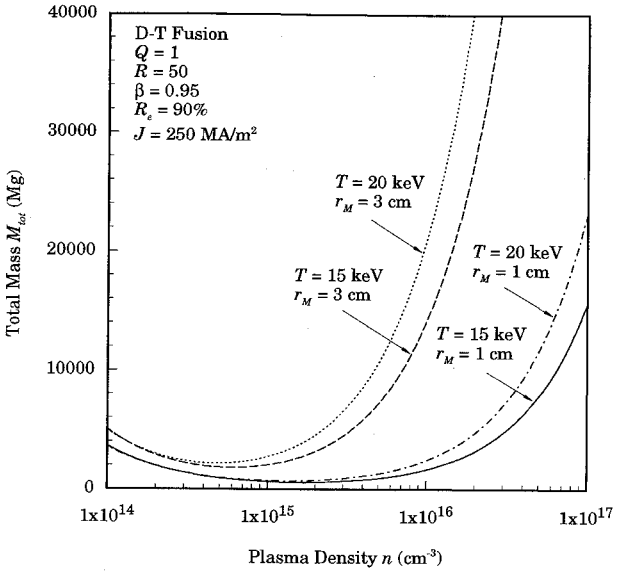

Fig. 8 Total rocket mass for advanced magnet technology.

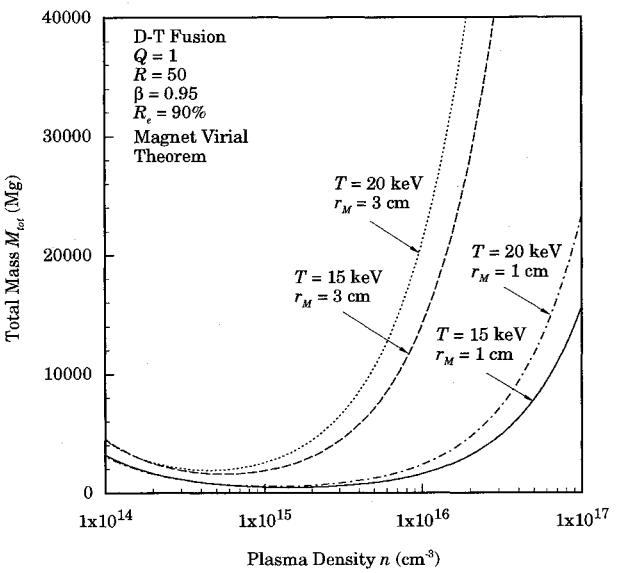

Fig. 9 Total rocket mass for magnets using virial theorem.

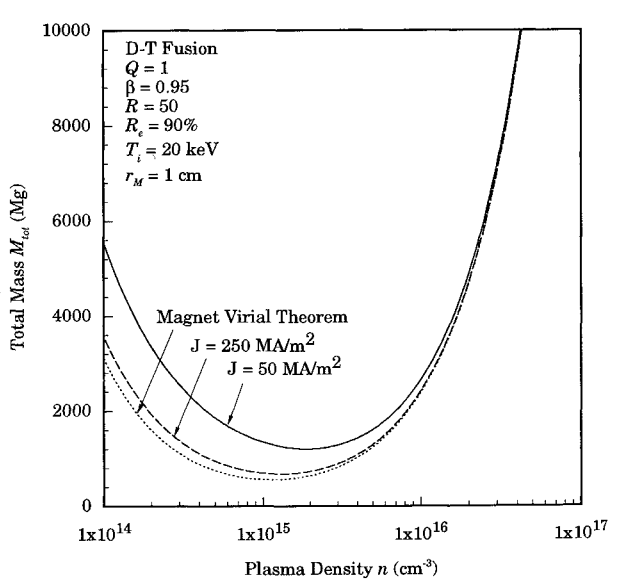

Fig. 10 Impact of magnet mass analysis on total mass of system.

Table 1a Mars mission with the gasdynamic D-T fusion rocket

	System 1	System 2	System 3	System 4
r_M, cm	1	3	1	3
n, cm^{-3}	10^{16}	10^{16}	10^{17}	10^{17}
T, keV	15	15	20	20
I_{sp}, s	1.58×10^5	1.58×10^5	1.82×10^5	1.82×10^5
F, N	2.52×10^4	2.26×10^5	3.36×10^5	3.02×10^6
m_f, mg, virial theorem magnet	1,611	14,138	22,348	209,950
m_f, mg, near-term magnet technology	1,847	14,412	23,487	210,113
τ_{RT}, days, virial theorem magnet	105.7	104.6	109.8	109.8
τ_{RT}, days, near-term magnet technology	113.0	105.6	110.1	109.9

Table 1b Effect of beta on travel time

Near-term magnet technology, J = 50 MA/m^2	β = 0.35	β = 0.50	β = 0.75	β = 0.95
M_{tot}, mg	2,062	1,969	1,886	1,847
τ_{RT}, days	117	117	114	113

Application to a Mars Mission

The true value of a propulsion device lies in its ability to provide safe travel in the shortest possible time for its crew. If we choose as an application for this gasdynamic fusion propulsion rocket a round-trip manned mission to Mars, and employ a continuous burn (constant thrust) acceleration/deceleration trajectory profile, then we can write for the round-trip travel time τ_{RT}[9]:

$$\tau_{RT} = (4D/gI_{sp}) + 4\sqrt{(Dm_f/F)} \tag{25}$$

The above equation can be derived by first using the standard rocket equation to calculate the outbound and return legs of a journey from point a to point b (and back again) along with the distances traveled. These are given by[10]

$$\tau_{ab} = \frac{I_{sp}}{F/W_f}\left(\frac{1}{\alpha^*}\right)\left(\frac{1}{\alpha} - 1\right) \tag{26}$$

$$\tau_{ba} = \frac{I_{sp}}{F/W_f}\left(\frac{1}{\alpha^*} - 1\right) \tag{27}$$

$$\tau_{RT} = \tau_{ab} + \tau_{ba} = \frac{I_{sp}}{F/W_f}\left(\frac{1}{\alpha\alpha^*} - 1\right) \tag{28}$$

$$D_{ab} = \frac{gI_{sp}^2}{F/W_f}\left(\frac{1}{\alpha^*}\right)\left(\frac{1}{\sqrt{\alpha}} - 1\right)^2 = D_{ba} \tag{29}$$

$$D_{ba} \frac{gI_{sp}^2}{F/W_f}\left(\frac{1}{\sqrt{\alpha^*}} - 1\right)^2 \tag{30}$$

where $W_f = gm_f$ is the dry weight, $1/\alpha = m_i/m_b$, m_i the initial mass ($m_b = m_f + m_p^{b\to a}$), and $1/\alpha^* = m_b/m_f$. Noting that $D_{ab} = D_{ba} \equiv D$, we can solve for α and α^* from Eqs. (29) and (30), and when we substitute the results in Eq. (28) we obtain the desired result, i.e., Eq. (25).

Assuming that the final mass is equal to the total propulsion system mass computed earlier (addition of a modest payload will not change the result very much), we observe from Eq. (25) that the travel time is more sensitive to I_{sp} than either m_f or F. Noting that D for an Earth-Mars mission is 0.78×10^{11} m, we can, using Eq. (25), calculate τ_{RT}, which we have done for several systems and summarized the results in Table 1a.

Table 2 Engineering parameters of a near-term gasdynamic D-T fusion rocket design

Q	1
β	0.95
R	50
R_e	0.9
n, m^{-3} (D + T)	10^{22}
T, keV	15
L, m	31.7
r_M, m	0.01
r_p, m	0.07
Halo thickness, m	0.10
Shield thickness, m	0.42
Shield-magnet gap, m	0.10
B_{p0}, T	11.3
E_s, GJ	2.41
v_{thi}, m/s	1.52×10^6
v_{the}, m/s	9.84×10^7
$v_{th,eff}$, m/s	1.54×10^6
F, N	2.52×10^4
$P_{F,eff}$, MW	3.89×10^4
P_f, MW	9562.5
P_b, MW	103.3
P_s, MW	53.1
P_n, MW	7660.9
Neutron wall load, MW/m^2	225.1
Surface heat flux, MW/m^2	4.6
J, MA/m^2	50.0
M_m, mg	188.8
M_{rad}, mg	1564.5
M_{ref}, mg	62.9
M_s, mg	31.9
M_{tot}, mg	1847.1
α_{eff}, kW/kg	21.0
$I_{sp,eff}$, s	1.58×10^5

The interesting observation that emerges from Table 1a is that the travel time for a Mars mission is not much different for the four systems, and more importantly, near-term magnet technology is not only adequate but perhaps more desirable. The reason for this is that the magnet mass is but a small part of the total mass, and it is overshadowed by the radiator mass that becomes very large when higher densities and temper-

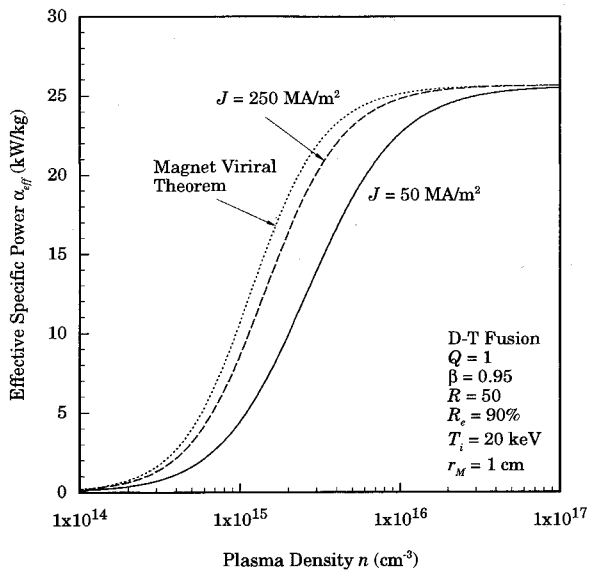

Fig. 11 Variation of rocket specific power with density for different magnet mass calculation.

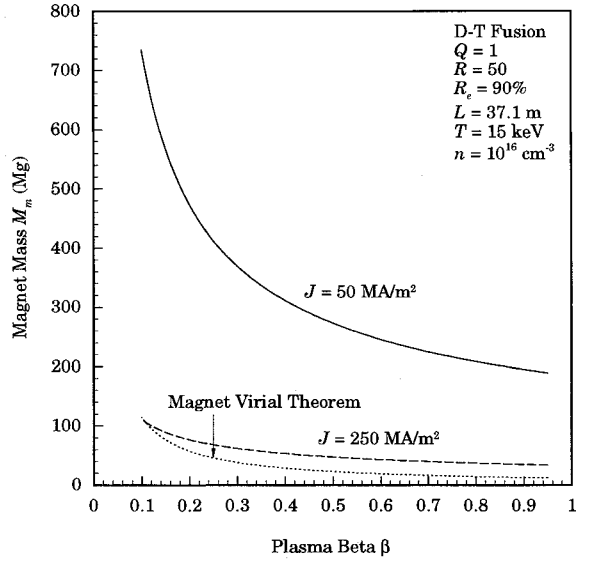

Fig. 12 Variation of magnet mass with plasma beta.

atures are used since they lead to larger neutron and radiation power. In fact, system 1 at a nozzle radius of 1 cm and almost present-day magnet technology should be especially suitable for a manned Mars mission, even though it requires a few more days than the other systems where technological demands are clearly more stringent. The relevant design parameters of that system are given in Table 2. Figure 11 further confirms the suitability of a propulsion system with a near-term technology, since it produces about the same specific power at $n = 10^{16}$ cm^{-3} as the more advanced systems.

All these results were obtained using a beta value of 0.95, which might be viewed as optimistic. It may be argued that a high degree of plasma stability may not be achievable, and hence, a more modest value of beta must be employed in assessing the performance of the rocket. We note from Eq. (6) that the vacuum magnetic field required to confine the plasma becomes larger at a smaller β, and that in turn means a more massive magnet. Clearly, that also means a larger total mass, and in an effort to assess the sensitivity of these quantities to β we have generated the results given in Figs. 12 and 13, in which the variations of the magnet mass and total mass with β are displayed, respectively. We note in both instances

Table 3 Engineering parameters of a near-term gasdynamic D-He^3 fusion rocket design

Q	1
β	0.95
R	50
R_e	0.9
n, m^{-3} (D + He^3)	1×10^{22}
n_D, m^{-3}	0.6×10^{22}
n_{He^3}, m^{-3}	0.4×10^{22}
T, keV	100
L, m	2857.9
r_M, m	0.01
r_p, m	0.07
Halo thickness, m	0.10
Shield thickness, m	0.19
Shield-magnet gap, m	0.10
B_{p0}, T	29.1
E_s, GJ	642.7
v_{thi}, m/s	3.93×10^6
v_{the}, m/s	2.08×10^8
$v_{th,eff}$, m/s	3.99×10^6
F, N	1.68×10^5
$P_{F,eff}$, MW	6.70×10^5
P_f, MW	5.32×10^5
P_b, MW	1.12×10^5
P_s, MW	1.18×10^5
P_n, MW	2.68×10^4
Neutron wall load, MW/m^2	8.7
Surface heat flux, MW/m^2	75.0
J, MA/m^2	50.0
M_m, mg	39,834.9
M_{rad}, mg	51,361.5
M_{ref}, mg	13,278.3
M_s, mg	906.5
M_{tot}, mg	105,381.2
α_{eff}, kW/kg	6.35
$I_{sp,eff}$, s	4.07×10^5

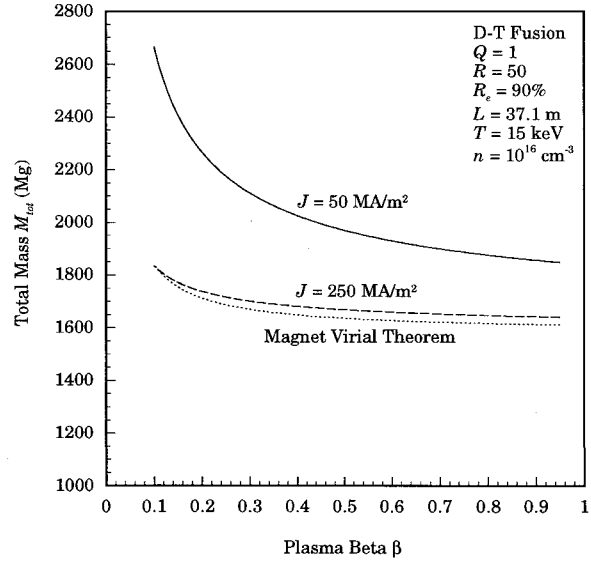

Fig. 13 Variation of total mass with plasma beta.

that the mass does not change dramatically for beta values larger than about 0.35, especially in the case of the superconducting magnets characterized by the high current density and the virial theorem. The variation is even less dramatic in the case of the total mass due to the fact that the magnet constitutes but a small fraction of all the components that make up the rocket dry mass. The sensitivity of travel time to β is given in Table 1b where the plasma parameters of Table 2 were used in obtaining the results shown. We readily note that less than 4% reduction in travel time is obtained

when the β value is nearly tripled (from 0.35 to 0.95). These differences will be even less distinguishable when advanced magnet technology is utilized. Current fusion experiments do make use of conventional cables that carry about 5 kA/cm^2 (i.e., 50 MA/m^2) in generating the magnetic fields utilized in confining the hot plasma. Some international devices (e.g., Tore Supra in France) are currently experimenting with the use of superconducting magnets for plasma confinement, and the likelihood of achieving very high current densities in the not too distant future does not appear unrealistic.

It has often been argued that better propulsion performance can be obtained if the D-T fuel is replaced by deuterium-helium (D-He^3) because of the significant reduction in neutron power, and correspondingly in radiator mass. Whereas neutron power constitutes about 80% of fusion power in D-T reactions, it constitutes about 5% in D-He^3 reactions, and such reduction should alleviate considerably problems associated with disposal of this heat component. The D-He^3 reaction itself does not produce neutrons, but the satellite reactions involving D do indeed produce neutrons, though to a lesser extent. These favorable aspects of D-He^3 reactions are, however, offset by the high ignition temperature required by this fuel cycle, and the corresponding large amount of synchrotron radiation emitted. For purposes of comparison we carried out analysis of system 1 (in Table 1a) for a D-He^3 fuel cycle at an operating temperature of 100 keV and the same plasma density of 10^{16} cm^{-3}. The results are summarized in Table 3. We note immediately that the rocket length increased from 32 m to a prohibitive length of about 2858 m, the confining magnetic field more than doubled, and even the neutron power more than tripled due to the significant increase in plasma volume. For the same reflection coefficient of 90% the synchrotron radiation power in the D-He^3 case is over 2000 times larger than its counterpart in the D-T case, resulting in a total propulsion mass that is well over 50 times larger. Because of the high temperature in the D-He^3 rocket, the specific impulse is about 2.5 times larger than its value in the D-T case, and the thrust is about 7 times larger, but because of the overwhelmingly larger total mass, the Mars mission will take three times as long to accomplish. If superconducting magnet design as reflected by magnet virial theorem is employed in place of present or near-term technology (J = 50 MA/m^2), the Mars mission travel time will be reduced by about 27%. In both instances, however, the specific power of the propulsion device is considerably smaller than its counterpart in the D-T case. In fact, even if the synchrotron radiation is totally neglected, the specific power in the D-He^3 case becomes comparable to that of D-T for present day magnet technology, but almost doubles if advanced technology is utilized.

Sensitivity to Rocket Mass

Because of the economics of putting objects in space it is clear that a total mass of 1847 mg using present day magnet technology (see Table 2) or even 1611 mg using future magnet technology (as given in Table 1a) may be prohibitively large, especially if it is to be assembled in space. We have, therefore, re-examined the governing equations of the system to see if other operating conditions might exist that could result in a more modest mass for the vehicle. The results presented earlier were chosen because they yielded the shortest length (as may be noted from the plots given in the text) without regard to the associated mass. If we do not insist on these plasma conditions that yield the smallest "L," and re-examine Eq. (11) to see if there exist other conditions that result in a significant reduction on the total mass, then the results given in Table 4 will emerge. These results reveal, in effect, the sensitivity of the total vehicle mass to the various plasma parameters that underlie the rocket performance. System 1 gives a summary of the relevant characteristics that result in minimal length, for mirror ratios of 50 and 100, whereas system 2 reflects an attempt to produce the smallest possible total mass without regard to the length. It should be noted that the results for system 2 were obtained without changing the previously used performance characteristics of the various components such as the radiator, shield, etc. We see that the rocket length increased substantially for system 2, whereas the confining magnetic field became smaller by almost a factor of 3. If we use the advanced magnet technology as the basis for computing the mass of this component we find that the total rocket mass is reduced to 400 and 295 mg for mirror ratios of 50 and 100, respectively. When compared to system 1, the thrust in system 2 is smaller due to the lower plasma density and temperature, and that in turn results in smaller thrust power and rocket specific power, although the latter quantity is still considered quite attractive at 11 and 14. If we apply these results to the Mars mission described earlier we find that the round-trip time has increased somewhat, but remains quite short compared to other propulsion systems. In short, this limited sensitivity study reveals that a more manageable rocket mass can indeed be attained with the gasdynamic mirror propulsion system, and there is no reason to believe that it cannot be reduced further if advances in radiator, shield, refrigerator, etc., technology are also achieved. As can be seen from Table 4, these reductions are feasible without seriously diminishing the propulsive capability of the system.

Summary and Conclusions

We have proposed and analyzed, in this article, a propulsion device with potentially attractive propulsive capabilities that, if realized, would lead to relatively short interplanetary travel times. It is based on the simple magnetic mirror fusion configuration that has been investigated extensively for decades for terrestrial power applications. Unlike those mirrors, however, where the plasma density is sufficiently low to be considered "collisionless," the proposed concept would contain a significantly higher density to justify identifying it as a highly collisional or a "gasdynamic" mirror in which the collision mean free path is considerably shorter than the length of the

Table 4 Sensitivity of rocket performance to total mass

	System 1		System 2	
Parameter	R = 50	R = 100	R = 50	R = 100
Rocket length, m	31.73	15.87	213	107
Plasma density, cm^{-3}	1×10^{16}	1×10^{16}	2×10^{15}	2×10^{15}
Plasma temperature, keV	15	15	10	10
Magnetic field, T	11.28	11.28	4.12	4.12
Thrust, N	2.52×10^4	2.52×10^4	3.36×10^3	3.36×10^3
Total mass,[a] mg	1611	1589	400	295
Specific impulse, s	1.58×10^5	1.58×10^5	1.29×10^5	1.29×10^5
Specific power, kW/kg	24	11	11	14
τ_{RT} to Mars, days	106	105	143	124

[a]Using advanced magnet technology.

system. Under these conditions plasma confinement is characterized by a confinement law that is drastically different from that which describes the collisionless mirror. Although, in the past, several authors considered the simple mirror machine as the engine of a hypothetical rocket, the results obtained are totally unrelated to those presented here since a collisionless mirror was used as the basis of their study.

We have seen that in the gasdynamic mirror rocket, large aspect ratio engines are desirable because of the associated better confinement that leads to a more efficient production of fusion energy, and the large degree of plasma stability that results in a more efficient utilization of the confining magnetic field. This is reflected in the high β value used in the analysis, which in turn resulted in relatively small magnet masses. However, as noted in this study, the magnet mass and, in turn, the total mass of the vehicle does not vary significantly over a wide range of β values, with the result that the travel time is hardly affected. Three magnet designs were examined, ranging from present day (or near-term) technology that utilizes windings that carry 50 MA/m^2, to an advanced (superconducting) technology that allows for much higher current densities. When applied to a round trip Mars mission that utilizes a continuous burn acceleration/deceleration trajectory profile, it is shown that a rocket that uses present day magnet technology can still make the round-trip in months instead of years.

An elementary design was also carried out in order to identify the major components of the system, their masses, and the demand placed on their performance capabilities. It is shown that next to the magnet mass the radiator mass constitutes the major portion of the total vehicle dry mass based on an assumed radiative capability of 5 MW/mg. When a D-T fuel is used to produce the fusion energy needed to propel the rocket, reasonable plasma and engineering parameters are found to characterize the system. For example, a magnetic field strength of about 11 T is shown to be adequate for plasma confinement, and that is slightly higher than ($\sim$10 T) the fields utilized in some present-day fusion experiments. In spite of the large vehicle mass of a DT-driven rocket, the thrust power generated is sufficiently high to produce an acceptable, if not an attractive, specific power.

A rocket that utilizes the D-He^3 fuel cycle was also examined in order to study the impact of an aneutronic (producing no neutrons) fuel on the performance of the rocket. A certain fraction of the fusion power did nevertheless appear in the neutrons due to the satellite reactions involving the deuterium, though to a much lesser extent. But because of the drastic increase in the operating temperature and size of the rocket, the total mass of the system increased dramatically over that of the D-T rocket, and the technological development demands of most of the components are so severe that realization of such a system in the foreseeable future appears to be at best remote.

Acknowledgment

This work was supported in part by the U.S. Department of Energy.

References

[1]Gerwin, R. A., et al., "Astronautics Laboratory Report," AL-TR-89-092, Feb. 1990.

[2]Kammash, T., *Fusion Reactor Physics—Principles and Technology*, Ann Arbor Publishers, Ann Arbor, MI, 1975, Chap. 4.

[3]Post, R. F., *Nuclear Fusion*, Vol. 27, 1987, p. 1579.

[4]Nagornyj, V. P., Ryutov, D. D., and Stupakov, G. V., *Nuclear Fusion*, Vol. 24, 1984, p. 1421.

[5]Hilton, J. L., Luce, J. S., and Thompson, A. S., "A Hypothetical Fusion Propulsion Rocket Vehicle," AIAA Paper 63-239, June 1963; also Hilton, J. L., *IEEE Transactions on Nuclear Science*, Vol. NS-10, No. 1, 1963, p. 153.

[6]Kilcrease, D. P., and Kirkpatrick, R. C., *Nuclear Fusion*, Vol. 28, 1988, p. 1465.

[7]Santarius, J. F., and Logan, B. G., AIAA Paper 93-2029, June 1993.

[8]Dolan, T. J., *Fusion Research, Technology*, Vol. III, Pergamon, New York, 1980.

[9]Kammash, T., 44th Congress of the International Astronautical Federation, IAF-93-S.3.472, Graz, Austria, Oct. 1993.

[10]Borowski, S. K., "A Comparison of Fusion/Antiproton Propulsion Systems For Interplanetary Travel," AIAA Paper 87-1814, June 1987.